Geometric Phase and Orbital Moment in Quantization Rules for Magnetic Breakdown

A. Alexandradinata and Leonid Glazman
Department of Physics, Yale University, New Haven, Connecticut 06520, USA
(Received 27 August 2017; published 19 December 2017)

The modern semiclassical theory of a Bloch electron in a magnetic field encompasses the orbital magnetization and geometric phase. Beyond this semiclassical theory lies the quantum description of field-induced tunneling between semiclassical orbits, known as magnetic breakdown. Here, we synthesize the modern semiclassical notions with quantum tunneling—into a single Bohr-Sommerfeld quantization rule that is predictive of magnetic energy levels. This rule is applicable to a host of topological solids with *unremovable* geometric phase, that also *unavoidably* undergo breakdown. A notion of topological invariants is formulated that nonperturbatively encode tunneling, and is measurable in the de Haas–van Alphen effect. Case studies are discussed for topological metals near a metal-insulator transition and overtilted Weyl fermions.

DOI: 10.1103/PhysRevLett.119.256601

The semiclassical Peierls-Onsager-Lifshitz theory [1–4] of a Bloch electron in a magnetic field has been extended [5–7] to incorporate two modern notions: a wave packet orbiting in quasimomentum ($\boldsymbol{k}$) space acquires a geometric Berry phase (ϕ_B) [8,9], as well as a second phase (ϕ_R) originating from the orbital magnetic moment of a wave packet about its center of mass [10,11]. Both ϕ_B and ϕ_R are evaluated on semiclassical orbits which are uniquely determined by Hamilton's equation. If the quasimomentum separation between two neighboring orbits is of the order of the inverse magnetic length, field-induced quantum tunneling (known as magnetic breakdown) [7,12–17] invalidates a unique semiclassical trajectory.

Can the modern semiclassical notions of geometric phase and orbital moment be combined with the quantum phenomenon of breakdown? A unified theory would describe a host of solids which have emerged in the recent intercourse between band theory and topology. These solids are characterized by geometric phase which is unremovable owing to symmetry; the robust intersection of orbits simultaneously guarantees breakdown.

We propose that the magnetic energy levels in these solids are determined by Bohr-Sommerfeld quantization rules that unify tunneling, geometric phase, and the orbital moment—these rules generalize the Onsager-Lifshitz-Roth quantization rules [2,4,6] for transport within a single band, and provide an algebraic method to calculate Landau-level spectra without recourse [18–20] to large-scale, numerical diagonalization. These rules are also predictive of de Haas–van Alphen [21,22] (dHvA) peaks, as well as of fixed-bias peaks of the differential conductance in scanning-tunneling microscopy (STM) [23,24].

While oscillatory patterns in the dHvA [21,22] measurement underlie the "fermiological" [25] construction of Fermi surfaces [26,27], such oscillations are generically disrupted by tunneling in low-symmetry solids [28]. Here, we demonstrate how multiharmonic oscillations may nevertheless persist in high-symmetry solids whose orbits intersect at a saddle point. Furthermore, the phase offset of each harmonic is a topological invariant that nonperturbatively encodes tunneling in magnetotransport, as well as sharply distinguishes Fermi surfaces with differing Berry phases.

Our last case study describes tunneling at the intersection of a hole and electron pocket, as exemplified by an overtilted Weyl point [29–33]; the corresponding magnetic energy levels were first studied numerically in Ref. [19]. Here, we present the first Berry-phase-corrected quantization rule which is valid at any tunneling strength, and compare our algebraically derived Landau-level spectra to their [19] numerically exact spectra.

Throughout this Letter, we orient the field along $\vec{z}$, such that orbits are contours of the band dispersion at fixed energy E and k_z. In the $\boldsymbol{k}^\perp \coloneqq (k_x, k_y)$ neighborhood where two orbits approach each other hyperbolically [illustrated in Fig. 1(a)], tunneling is significant if the rectangular area $(4ab)$ inscribed between the hyperbolic arms is comparable to or smaller than $1/l^2$, with $l \coloneqq (\hbar c/e|\boldsymbol{B}|)^{1/2}$ the magnetic length. The orientation of the approaching orbits, as determined by Hamilton's equation $\hbar\dot{\boldsymbol{k}} = -|e|\boldsymbol{v}\times\boldsymbol{B}/\hbar c$, distinguishes between two qualitatively distinct types of breakdown: (a) if both arms carry the same orientation, tunneling occurs between contours of the same band. Case (b) for which both arms are oppositely oriented will be discussed in the second half of the letter. The former case, known as intraband breakdown, occurs wherever band contours change discontinuously as a function of energy; the nucleus of this Lifshitz transition is a saddle point which disperses as $\varepsilon_{\boldsymbol{k}} = k_x^2/2m_1 - k_y^2/2m_2$. The vanishing band velocity at $\boldsymbol{k}^\perp = \boldsymbol{0}$ implies that a hypothetical wave packet satisfying Hamilton's equation never reaches the saddle

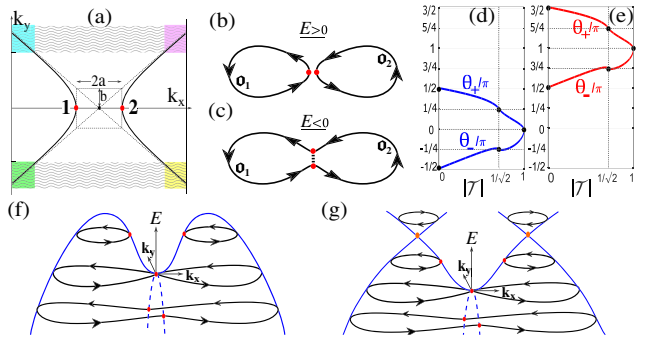

FIG. 1. (a) Illustration of a region in $\boldsymbol{k}^\perp$ space with significant tunneling. (b)–(c) Constant-energy band contours of two distinct orbits (above the saddle point) that merge into one (below). Black arrows indicate the orientation determined by Hamilton's equation. (d)–(e) Plot of θ_η vs $|\mathcal{T}| = (1+e^{-2\pi\mu})^{-1/2}$ for the conventional metal (blue line) and the topological metal (red). (f)–(g) Band dispersion of a conventional metal (left), and a topological metal (right).

point in finite time [34]. The probability of vertical transmission (between ↗-incoming and ↖-outgoing trajectories) equals $|\mathcal{T}|^2 \coloneqq (1+e^{-2\pi\mu})^{-1}$ [35], with $\mu \coloneqq \sqrt{m_1 m_2} E l^2$ geometrically interpreted as $abl^2/2$, and E measured from the saddle point.

The conceptually simplest realization of intraband breakdown occurs for two orbits (at $E>0$) that merge into a single orbit (at $E<0$), as illustrated in Figs. 1(b)–1(c). This merger has at least two topologically distinct realizations: (ai) a conventional metal whose band dispersion has two nearby maxima [Fig. 1(f)], and (aii) a topological metal near a metal-insulator transition, where two Weyl points (touching points between two conically dispersing bands) [36,37] with opposite chirality are near annihilation [Fig. 1(g)]. Our comparative study of (ai)–(aii) illustrates how their difference in Berry phase manifests in their Landau levels, which are determined in both cases by the following quantization rule:

$$\cos\left[\left.\frac{\Omega_1+\Omega_2}{2}\right|_{E,l^2}+\varphi(\mu)\right]=|\mathcal{T}(\mu)|\cos\left[\left.\frac{\Omega_1-\Omega_2}{2}\right|_{E,l^2}\right]. \quad (1)$$

$\mathcal{T} \coloneqq (1+e^{-2\pi\mu})^{-1/2}e^{i\varphi}$ is the aforementioned transmission amplitude, with $\varphi = \arg[\Gamma(1/2-i\mu)] + \mu\log|\mu| - \mu$ involving the Γ function [38]. $\Omega_j \coloneqq \Omega[\mathfrak{o}_j]$ is the semiclassical phase acquired by a wave packet in traversing $\mathfrak{o}_j$, which is a closed Feynman trajectory illustrated in Figs. 1(b)–1(c). For $E>0$, $\mathfrak{o}_1$ is simply the left orbit in Fig. 1(b); for $E<0$, $\mathfrak{o}_1$ combines the left half of the orbit with a tunneling trajectory [dashed line in Fig. 1(c)] through the semiclassically forbidden region,

$$\Omega[\mathfrak{o}_j(E), l^2] = l^2 S[\mathfrak{o}_j(E)] + \phi_M + \lambda[\mathfrak{o}_j(E)], \quad (2)$$

includes (i) a dynamical phase proportional to the $\boldsymbol{k}^\perp$-space area S bounded by $\mathfrak{o}_j$, with S positive (negative) for a clockwise-oriented (anticlockwise) orbit. Here, $\{S[\mathfrak{o}_j]\}$ carry the same sign.

The remaining contributions to Ω_j are subleading in powers of $|\boldsymbol{B}|$: (ii) the Maslov phase (ϕ_M) equals π for trajectories that are deformable to a circle [39], and (iii) a further correction (λ) encodes the aforementioned geometric phase and orbital moment, as well as the well-known Zeeman coupling. Whether the orbital moment contributes to λ depends on the crystalline symmetries of the spin-orbit-coupled solid, as well as the field alignment relative to certain crystallographic axes. First consider a time-reversal invariant, noncentrosymmetric metal with a twofold rotational axis parallel to the field ($\vec{z}$)—these symmetries stabilize Weyl points in the rotationally invariant two-torus (denoted $BT_\perp$) [31]. Then, $\lambda_j \coloneqq \lambda[\mathfrak{o}_j]$ equals the geometric phase (ϕ_B), i.e., the line integral over $\mathfrak{o}_j$ of the Berry one-form [8] $i\langle u_{1\boldsymbol{k}}|\nabla_{\boldsymbol{k}}u_{1\boldsymbol{k}}\rangle\cdot d\boldsymbol{k}$. Here, $e^{i\boldsymbol{k}\cdot\boldsymbol{r}}u_{1\boldsymbol{k}}$ is the Bloch function of the low-energy band in Figs. 1(f)–1(g); redefining $u_{1\boldsymbol{k}}$ by a $\boldsymbol{k}$-dependent phase may add to ϕ_B an integer multiple of 2π, but does not affect the quantization condition in Eq. (1). The composition of time-reversal and twofold rotation is a symmetry (denoted $T\mathfrak{c}_{2z}$) that makes wave functions real at each $\boldsymbol{k}^\perp \in BT_\perp$, hence, $e^{i\phi_B} \in \mathbb{R}$ [40], with $\phi_B = 0$ and π for the conventional and topological metal, respectively. Moreover, since the z component of angular momentum flips under $T\mathfrak{c}_{2z}$, both the orbital moment and the spin expectation value $[\boldsymbol{s}(\boldsymbol{k})]$ lie parallel to $BT_\perp$, and do not contribute to λ [41].

To observe the orbital moment and Zeeman coupling, we consider a different class of solids with a mirror symmetry ($x \to -x$) that relates the two maxima in (ai) and the two Weyl points in (aii); this symmetry allows the orbital moment/$\boldsymbol{s}$ to tilt out of $BT_\perp$ at $\boldsymbol{k}^\perp$ which are not reflection invariant. Then, $\lambda = \phi_B + \phi_R + \phi_Z$ [42], with ϕ_R defined as the line integral [44] of the orbital-moment one-form [41]:

$$\mathfrak{A}\cdot d\boldsymbol{k} = i\sum_{l\neq 1}\langle u_{1\boldsymbol{k}}|\nabla_{\boldsymbol{k}}u_{l\boldsymbol{k}}\rangle\Pi^y_{l1}dk_x/2v_y + (x\leftrightarrow y). \quad (3)$$

Here, $\boldsymbol{\Pi}(\boldsymbol{k})_{ln} \coloneqq i\langle u_{l\boldsymbol{k}}|e^{-i\boldsymbol{k}\cdot\hat{\boldsymbol{r}}}[\hat{H}_0,\hat{\boldsymbol{r}}]e^{i\boldsymbol{k}\cdot\hat{\boldsymbol{r}}}|u_{n\boldsymbol{k}}\rangle/\hbar$ are matrix elements of the velocity operator, $\boldsymbol{v} \coloneqq \boldsymbol{\Pi}_{11}$, $\hat{H}_0$ is the single-particle, translation-invariant Hamiltonian, and $\hat{\boldsymbol{r}}$ the position operator. $\sum_{l\neq 1}$ denotes a sum over all bands excluding $u_{1\boldsymbol{k}}$ [45]. Finally, λ is contributed by the Zeeman phase (ϕ_Z), which is the line integral [46] of $g_0 s_z(\boldsymbol{k})|d\boldsymbol{k}|/2m(v_x^2+v_y^2)^{1/2}$, with $g_0 \approx 2$ the free-electron g factor, and m the free-electron mass. If the orbital moment/$\boldsymbol{s}$ tilts toward $+\vec{z}$ at a wave vector $\boldsymbol{k}^\perp \in \mathfrak{o}_1$, the tilt occurs toward $-\vec{z}$ in the reflection-mapped wave vector lying in $\mathfrak{o}_2$, hence $\lambda_1 = -\lambda_2$ modulo 2π [47].

The quantization rule [Eq. (1)] has been derived by Azbel [13] in the Peierls-Onsager approximation [1–3], which effectively dispenses with the λ correction to Ω. By accounting for the subleading-in-$|\boldsymbol{B}|$ correction [5–7] to the effective Hamiltonian of a Bloch electron in a magnetic

field, we have derived an improved connection formula [43] that patches the semiclassical WKB wave function [48,49] across the region of strong tunneling. Continuity of the patched WKB wave function imposes the λ-corrected quantization rule in Eq. (1).

Viewing Eq. (1) at fixed field, the discrete energetic solutions correspond to Landau levels. Viewed at constant Fermi energy (E_F), the discrete solutions correspond to values of l^2, where Landau levels successively become equal to E_F, leading to peaks in a dHvA or fixed-bias STM measurement; such discrete l^2 are, henceforth, referred to as dHvA levels. The Landau and dHvA levels may be intuited in the semiclassical limit: $\mu \to \infty$, where $\mathcal{T} \to 1$, and Eq. (1) simplifies to independent quantization rules for two uncoupled orbits $\mathfrak{o}_j$ illustrated in Fig. 1(b): $\Omega_j/2\pi \in \mathbb{Z}$. The Landau spectrum splits into two sets labeled by j, where adjacent spacings within each set are locally periodic as $E_{j,n+1} - E_{j,n} = 2\pi/[l^2(\partial S_j/\partial E)]$ with the right-hand side evaluated at $E_{j,n}$, $n \in \mathbb{Z}$ and $S_j := S[\mathfrak{o}_j]$. Analogously, the dHvA levels split into two sets, where adjacent levels in each set are periodic as $l^2_{j,n+1} - l^2_{j,n} = 2\pi/S_j(E_F)$. This (local) periodicity also characterizes the opposite semiclassical limit $\mu \to -\infty$, where both $\mathcal{T}$ and $\varphi \to 0$, and we obtain a single quantization rule for the merged orbit $\mathfrak{o}_1 + \mathfrak{o}_2$ illustrated in Fig. 1(c). Let us describe the case of general μ in symmetry classes where the two orbits are not mutually constrained (this includes the Tc_{2z} class): the two incommensurate harmonics $(\Omega_1 \pm \Omega_2)/2$ in Eq. (1) competitively produce a Landau and dHvA spectrum that is not (locally) periodic but retains a long-ranged correlation; such spectra have been called quasirandom [28].

In contrast, the mirror symmetry in the second class of solids enforces $S[\mathfrak{o}_1] = S[\mathfrak{o}_2] := S$ at all energies, and this demonstrably allows for locally periodic spectra. The mirror-symmetric quantization condition is solved by two sets of Landau-dHvA levels distinguished by an index $\eta \in \pm$: $l^2|S(E)| = 2\pi n + \phi_M + \theta_\eta$, with

$$\theta_\eta(E, l^2) := \varphi(\mu) + \cos_\eta^{-1}[|\mathcal{T}(\mu)|\cos(\lambda_1)], \qquad (4)$$

defined as a phase: $\theta \sim \theta + 2\pi$, and $\cos_\eta^{-1}(\cdot)$ denotes the principal value in $[0, \pi]$ for $\eta = +$, and in $[-\pi, 0]$ for $\eta = -$. For $\mu \to \infty$, $\theta_\pm \to \pm\lambda_1$ implies symmetrically split Landau levels; as $\mu \to -\infty$, $\theta_\pm \to \pm\pi/2$ implies that this symmetric splitting equals π, and both sets of Landau levels (distinguished by η) may be viewed as a single set with an emergent local period $2\pi/[l^2\partial(2S)/\partial E]$—this corresponds to a combined orbit that is intersected by a reflection-invariant line; $S[\mathfrak{o}_1 + \mathfrak{o}_2] = 2S$, and $\lambda[\mathfrak{o}_1 + \mathfrak{o}_2] = 0$ [50]. To observe locally periodic dHvA levels at E_F, it is necessary that θ varies slowly on the scale of the dHvA period $2\pi/S(E_F)$. Indeed, the typical scale of variation for $|\mathcal{T}(\mu)|$ and $\varphi(\mu)$ is $\Delta\mu \sim 1$, which implies a scale $\Delta l^2 \sim 1/\sqrt{m_1 m_2}E_F$ from the definition of μ; $\Delta l^2/[2\pi/S(E_F)]$ is, therefore, negligible for small enough $|E_F|$ or large enough $S(E_F)$. Presuming these conditions, θ_η is extractable as a phase offset in the dHvA oscillations [41]. Equation (4) represents one key result for intraband breakdown—that the dHvA phase offset nonlinearly depends on both the tunneling parameter $\mathcal{T}$, as well as the semiclassical phase corrections: ϕ_R, ϕ_B, ϕ_Z.

To conclude our discussion of intraband breakdown, we propose a symmetry class where θ depends on a universal function of μ, with an additive Berry-phase correction that is insensitive to symmetric deformations of the metal. In addition to the mirror symmetry presupposed in Eq. (4), we further impose Tc_{2z} symmetry so that $e^{i\lambda} = e^{i\phi_B} = 1$ (-1) for the conventional (topological) metal; this is the symmetry class of TaAs, which has four mirror-related pairs [51] of Weyl points in the rotational-invariant $BT_\perp$ [52–54]. Equation (4) thus simplifies to $\theta_\eta = \varphi(\mu) + \cos_\eta^{-1}|\mathcal{T}(\mu)| + \phi_B$, which are plotted against $|\mathcal{T}(\mu)|$ in Figs. 1(d)–1(e), for both topological (red line) and conventional (blue) metals. As μ is varied over $\mathbb{R}$, θ_η robustly covers the interval $[\pi/2, 3\pi/2]$ in the former case, and $[-\pi/2, \pi/2]$ in the latter; the exact π offset originates from the Berry-phase difference. In both cases, $\theta_+ = \theta_-$ for $\mu \to \infty$ implies a twofold degeneracy in the Landau levels, which did not arise in the Tc_{2z}-asymmetric case. We, therefore, associate the robust covering of a π interval (in either case) to a Lifshitz transition in solids with Tc_{2z} and mirror symmetries. This may be viewed in a unifying analogy with field-free topological insulators, where the Berry phase covers 2π [55–61] (or rational fractions thereof) [62,63] as a function of a crystal wave vector. In comparison, θ_η includes not just the Berry phase, but also nonperturbatively encodes tunneling through its dependence on $\mathcal{T}$. Being robust against symmetry-preserving deformations of the metal, the π covering of θ_η may be viewed as a topological invariant in quantum magnetotransport.

In case (b), both hyperbolic arms are oppositely oriented and belong to distinct bands—they touch at the intersection of hole- and electronlike pockets, as exemplified by an overtilted Weyl fermion [29–31,33]. This touching point is modeled by the Hamiltonian: $H_{II}(\boldsymbol{k}^\perp) = (u + v\sigma_3)k_x + w\sigma_1 k_y$, with $|u| > |v|$ and σ_j Pauli matrices. Interband tunneling occurs with the Landau-Zener probability $e^{-2\pi\bar{\mu}}$ [7], with $\bar{\mu} = (vEl)^2/2|w|(u^2 - v^2)^{3/2}$, and E measured from the degeneracy. This probability is unity at $E = 0$; in comparison, $|\mathcal{T}|^2 = 1/2$ at the saddle point [35]. In both intra- and interband breakdown, the respective dimensionless parameters $|\mu|$ and $\bar{\mu}$ are geometrically interpreted as $abl^2/2$; however, a and b are distinct functions of E and $\boldsymbol{k}\cdot\boldsymbol{p}$ parameters: u, v, w in H_{II}, and m_1, m_2 for the saddle point.

The simplest scenario [19] of two orbits $\{\bar{\mathfrak{o}}_j\}_{j=1}^2$ linked by interband breakdown describes an overtilted Weyl fermion modelled by $H(\boldsymbol{k}^\perp) = H_{II} - |t|(1 - \sigma_3)k_x^3$; such

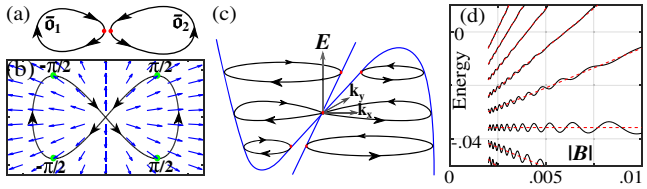

FIG. 2. An overtilted Weyl point that is not linked by tunneling to other Weyl points. (a) Band contours at fixed nonzero energy. (b) Zero-energy band contour of $H_{II} - |t|(1-\sigma_3)k_x^3 := d_1(\boldsymbol{k}^\perp)\sigma_1 + d_3(\boldsymbol{k}^\perp)\sigma_3$; the $\boldsymbol{d}$-vector is illustrated by blue arrows, with d_1 (d_3) the vertical (horizontal) component of each arrow. (c) Band dispersion. (d) Landau spectrum for the tight-binding model in Ref. [19], employing their units for energy and $|\boldsymbol{B}|$.

fermions were predicted to arise in WTe_2 [31], whose symmetry class (Tc_{2z}) we adopt in the following discussion [64]. The corresponding constant-energy band contours are illustrated in Figs. 2(a)–2(c), and the quantization condition is

$$\cos\left[\left.\frac{\Omega_{\bar{1}}+\Omega_{\bar{2}}}{2}\right|_{E,l^2}\right] = \tau(\bar{\mu})\cos\left[\left.\frac{\Omega_{\bar{1}}-\Omega_{\bar{2}}}{2}\right|_{E,l^2} + \bar{\varphi}(\bar{\mu})\right], \quad (5)$$

where $\tau e^{i\bar{\varphi}}$ (with $\tau := \sqrt{1-e^{-2\pi\bar{\mu}}}$) is the amplitude for intraband transmission between $\searrow$-incoming and $\swarrow$-outgoing trajectories, and $\bar{\varphi} = \bar{\mu} - \bar{\mu}\ln\bar{\mu} + \arg[\Gamma(i\bar{\mu})] + \pi/4$. $\Omega_{\bar{j}}$ is the phase acquired by a wave packet in traversing the closed Feynman trajectory $\bar{\mathfrak{o}}_j$ in Fig. 2(a). $\Omega_{\bar{j}} := \Omega[\bar{\mathfrak{o}}_j]$ has the same functional form as Eq. (1), with $e^{i\lambda} = e^{i\phi_B} \in \mathbb{R}$ owing to Tc_{2z} symmetry; $e^{i\phi_B}$ changes discontinuously across the band-touching point, owing to $\bar{\mathfrak{o}}_1$ encircling the Dirac point only for positive energies. The opposing orientations of $\{\bar{\mathfrak{o}}_j\}$ result in $\{S[\bar{\mathfrak{o}}_j]\}$ carrying different signs.

Equations (5) and (2) is our central result for interband breakdown, and may be derived from eigensolution of the effective Hamiltonian $\mathcal{H} = (u + v\sigma_3)K_x + w\sigma_1 K_y$ in the vicinity of the band-touching point, with kinetic quasimomentum operators satisfying $\boldsymbol{K}\times\boldsymbol{K} = i|e|\boldsymbol{B}/c$; $\mathcal{H}$ is written in a representation whose basis functions are magnetic analogs [17] of Luttinger-Kohn functions [65]. From $\mathcal{H}$ we derive an improved connection formula [43] which extends a previous work [17] by including the effect of the Berry phase; continuity of the connected WKB wave function then imposes Eqs. (5) and (2).

Since no crystalline symmetry relates an electron to a hole pocket, the two harmonics $(\Omega_{\bar{1}} \pm \Omega_{\bar{2}})/2$ in Eq. (5) are generically incommensurate, and competitively produce a quasirandom Landau-dHvA spectrum. There are two semiclassical limits where a locally periodic spectrum emerges: (i) for $\bar{\mu} \gg 1$ (the weak-field limit above or below the Dirac-point energy), the intraband-transmission amplitude $\tau e^{i\bar{\varphi}} \to 1$, and we obtain independent quantization conditions $\Omega_{\bar{j}} = 2n\pi$ for two uncoupled orbits. (ii) For $\bar{\mu} \approx 0$, the interband-tunneling probability approaches unity, and Eq. (5) is solved approximately by

$$l^2(S_{\bar{1}} + S_{\bar{2}})|_{E_n^0} = 2n\pi; \qquad S_{\bar{j}} := S[\bar{\mathfrak{o}}_j], \qquad n \in \mathbb{Z}. \quad (6)$$

One subtlety of the limit $\bar{\mu} \to 0$ is that $\Omega_{\bar{j}}$ is well-defined only for isolated orbits [cf. Eq. (2)]. At the Dirac-point energy, the two orbits merge into a figure of eight illustrated in Fig. 2(b), and the Berry connection (for a $\boldsymbol{k}$-derivative in the azimuthal direction) diverges at $\boldsymbol{k}^\perp = 0$ [66]. The validity of Eq. (6) at strictly-zero energy may independently be justified by the following semiclassical quantization rule: to leading order in $|\boldsymbol{B}|$, Eq. (6) may be reinterpreted as a generalization of the Onsager-Lifshitz rule [2,4] to an orbit which is only partially electronlike [19,20]. The field-independent correction to Eq. (6) comprises ϕ_M and ϕ_B, which *individually* vanish; this contradicts a claim [19] that $\phi_M = \phi_B = \pi$. That ϕ_B vanishes following from inspection of Fig. 2(b): by following the figure-of-eight trajectory, the wave function pseudospin does not wind. ϕ_M may be derived from the connection formulas of turning points where the WKB wave function is invalid [48]. The connection phase at each point is $\pm\pi/2$, with $\pm$ determined by the orientation of a wave packet as it rounds the point [43]. $\phi_M = 0$ follows from the vanishing of the net connection phase [green dots in Fig. 2(b)].

Let us perturbatively treat quasirandom Landau-dHvA spectra in parameter regimes, where a single harmonic is dominant. For $\bar{\mu} \approx 0$, the dominant harmonic is associated to the semiclassical fan: $\{E_n^0(B)\}_{n\in\mathbb{Z}}$ [cf. Eq. (6)]; to leading order in τ, the tunneling correction to the fan oscillates with the frequency of the weaker harmonic:

$$\delta E_n^1 = 2(-1)^{n+1}\mathrm{sgn}[E]\frac{\tau(\bar{\mu})}{l^2(S_{\bar{1}}+S_{\bar{2}})'}\sin\left[\frac{l^2(S_{\bar{1}}-S_{\bar{2}})}{2} + \bar{\varphi}\right], \quad (7)$$

with the right-hand side evaluated at E_n^0, and $O' := \partial O/\partial E$. The tunneling correction to E_0^0 (where the zero-field electron and hole pockets are perfectly compensated) is linear in E_0^0 and grows as $|\boldsymbol{B}|^{1/2}$ to lowest order in $|\boldsymbol{B}|$. As $|E| \to 0$, there is a logarithmic divergence in the second-order derivatives (with respect to E) of the classical action function $[l^2(S_{\bar{1}} - S_{\bar{2}})]$; in Eq. (7), this nonanalyticity is canceled by a logarithmic divergence in the tunneling phase $\bar{\varphi}$. While the Berry phase did not affect the semiclassical fan of Eq. (6), it shifts the phase of the tunneling correction (δE_n^1) by $\pi/2$; this has already been accounted for in Eq. (7). The validity of Eq. (7) relies on τ and $\bar{\varphi}$ being small and slowly varying on the scale of δE_n^1. Indeed, the typical scale of variation for τ and $\bar{\varphi}$ is $\Delta\bar{\mu} \sim 1$, which implies an scale $\Delta E \sim \sqrt{w}(u^2 - v^2)^{3/4}/(vl)$. For typical values of u and v, $\delta E_n^1/\Delta E$ vanishes for small enough field or $|E_n^0|$.

Our perturbation theory [Eqs. (6), (7)] is tested against the numerically exact Landau levels of an overtilted Weyl point modeled in Ref. [19]. Inserting their tight-binding parameters (detailed in the Supplemental Material [67]) into Eqs. (6)–(7), we plot in Fig. 2(d) the semiclassical fan [dashed lines] and the quantum correction [solid], which compares favorably with Fig. 2 in Ref. [19].

Discussion.—We have presented generalized quantization rules that incorporate both tunneling and the geometric phase. Because of the intrinsic phase ambiguity in the wave function of wave packets that approach or leave a tunneling region, we broadly argue that the geometric phase should manifest in any tunneling phenomena. This phase is especially relevant if tunneling occurs within a subspace of states (bands, in our context) nontrivially embedded in a larger Hilbert space; this has been overlooked in conventional treatments [13,17,68] of tunneling by connection formulas.

The modern prototype of a nontrivially embedded band is one that disperses conically near a band-touching (Dirac-Weyl) point. We have exemplified how the unremovable geometric phase of a Dirac-Weyl point influences the quantization rules for both intra- [cf. Eqs. (1), (2)] and interband [cf. Eqs. (5), (2)] breakdown; consequences have been discussed for the spectra of Landau levels and dHvA peaks.

The authors are grateful to T. O'Brien for clarifying his numerical calculation. We acknowledge support by the Yale Postdoctoral Prize Fellowship and NSF DMR Grant No. 1603243.

[1] R. Peierls, Z. Phys. **80**, 763 (1933).
[2] L. Onsager, London Philos. Mag. J. Sci. **43**, 1006 (1952).
[3] J. M. Luttinger, Phys. Rev. **84**, 814 (1951).
[4] L. M. Lifshitz and A. Kosevich, Dokl. Akad. Nauk SSSR **96**, 963 (1954).
[5] W. Kohn, Phys. Rev. **115**, 1460 (1959).
[6] L. Roth, J. Phys. Chem. Solids **23**, 433 (1962).
[7] E. I. Blount, Phys. Rev. **126**, 1636 (1962).
[8] M. V. Berry, Proc. R. Soc. A **392**, 45 (1984).
[9] G. P. Mikitik and Y. V. Sharlai, Phys. Rev. Lett. **82**, 2147 (1999).
[10] M.-C. Chang and Q. Niu, Phys. Rev. B **53**, 7010 (1996).
[11] M. Wilkinson and R. J. Kay, Phys. Rev. Lett. **76**, 1896 (1996).
[12] M. H. Cohen and L. M. Falicov, Phys. Rev. Lett. **7**, 231 (1961).
[13] M. Y. Azbel, J. Exp. Theor. Phys. **12**, 891 (1961).
[14] A. B. Pippard, Proc. R. Soc. A **270**, 1 (1962).
[15] A. B. Pippard, Phil. Trans. R. Soc. A **256**, 317 (1964).
[16] W. G. Chambers, Phys. Rev. **149**, 493 (1966).
[17] A. Slutskin, J. Exp. Theor. Phys. **26**, 474 (1968).
[18] M. Serbyn and L. Fu, Phys. Rev. B **90**, 035402 (2014).
[19] T. E. O'Brien, M. Diez, and C. W. J. Beenakker, Phys. Rev. Lett. **116**, 236401 (2016).
[20] M. Koshino, Phys. Rev. B **94**, 035202 (2016).
[21] W. J. de Haas and P. M. van Alphen, Proceedings of the Rochester Academy of Science **33**, 1106 (1930).
[22] L. W. Shubnikov and W. J. de Haas, Proceedings of the Rochester Academy of Science **33**, 130 (1930).
[23] S. Jeon, B. B. Zhou, A. Gyenis, B. E. Feldman, I. Kimchi, A. C. Potter, Q. D. Gibson, R. J. Cava, A. Vishwanath, and A. Yazdani, Nat. Mater. **13**, 851 (2014).
[24] I. Zeljkovic, Y. Okada, M. Serbyn, R. Sankar, D. Walkup, W. Zhou, J. Liu, G. Chang, Y. J. Wang, M. Z. Hasan, F. Chou, H. Lin, A. Bansil, L. Fu, and V. Madhavan, Nat. Mater. **14**, 318 (2015).
[25] D. Shoenberg, *Magnetic Oscillations in Metals* (Cambridge University Press, Cambridge, England, 1984).
[26] N. W. Ashcroft and N. D. Mermin, *Solid State Physics* (Thomson Learning, Connecticut, USA, 1976).
[27] T. Champel and V. P. Mineev, Philos. Mag. B **81**, 55 (2001).
[28] M. Kaganov and A. Slutskin, Phys. Rep. **98**, 189 (1983).
[29] H. Isobe and N. Nagaosa, Phys. Rev. Lett. **116**, 116803 (2016).
[30] E. J. Bergholtz, Z. Liu, M. Trescher, R. Moessner, and M. Udagawa, Phys. Rev. Lett. **114**, 016806 (2015).
[31] A. A. Soluyanov, D. Gresch, Z. Wang, Q. Wu, M. Troyer, X. Dai, and B. A. Bernevig, Nature (London) **527**, 495 (2015).
[32] Y. Xu, F. Zhang, and C. Zhang, Phys. Rev. Lett. **115**, 265304 (2015).
[33] L. Muechler, A. Alexandradinata, T. Neupert, and R. Car, Phys. Rev. X **6**, 041069 (2016).
[34] A. M. Kosevich, Low Temp. Phys. **30**, 97 (2004).
[35] E. C. Kemble, Phys. Rev. **48**, 549 (1935).
[36] H. B. Nielsen and M. Ninomiya, Nucl. Phys. **B193**, 173 (1981).
[37] X. Wan, A. M. Turner, A. Vishwanath, and S. Y. Savrasov, Phys. Rev. B **83**, 205101 (2011).
[38] $|\varphi|$ is bounded by 0.05π.
[39] J. B. Keller, Ann. Phys. (N.Y.) **4**, 180 (1958).
[40] Each orbit falls into symmetry class [I, $s = 0$] in the tenfold classification of Ref. [41], where the resultant symmetry constraints on the Berry phase, orbital moment, and Zeeman effect are explained in full generality.
[41] A. Alexandradinata, C. Wang, W. Duan, and L. Glazman, arXiv:1707.08586.
[42] The present form of Ω_j presupposes a reflection symmetry; the most general form of Ω_j is clarified in a separate publication [43].
[43] The first-order-corrected connection formulas for both intra- and interband breakdown is presented in a separate, mathematically oriented work; A. Alexandradinata and L. Glazman (to be published).
[44] The integral is over $\mathfrak{o}_j$ without the tunneling trajectory.
[45] These other bands are not illustrated in Fig. 1(f) but exist as a matter of principle; in Fig. 1(g), only one other band is illustrated.
[46] See Ref. [44].
[47] Both orbits collectively fall into symmetry class [II-B, $s = 0$, $u = 1$] in Ref. [40].
[48] G. Zil'berman, J. Exp. Theor. Phys. **5**, 208 (1957).
[49] H. J. Fischbeck, Phys. Status Solidi B **38**, 11 (1970).
[50] This orbit falls into class [II-A, $u = 1$, $s = 0$] in Ref. [41].

[51] The orbits in TaAs may not resemble the ones illustrated in Fig. 1(g), and a different quantization condition may be appropriate for TaAs [43].
[52] H. Weng, C. Fang, Z. Fang, B. A. Bernevig, and X. Dai, Phys. Rev. X **5**, 011029 (2015).
[53] B. Q. Lv, H. M. Weng, B. B. Fu, X. P. Wang, H. Miao, J. Ma, P. Richard, X. C. Huang, L. X. Zhao, G. F. Chen, Z. Fang, X. Dai, T. Qian, and H. Ding, Phys. Rev. X **5**, 031013 (2015).
[54] S.-Y. Xu, I. Belopolski, N. Alidoust, M. Neupane, G. Bian, C. Zhang, R. Sankar, G. Chang, Z. Yuan, C.-C. Lee, S.-M. Huang, H. Zheng, J. Ma, D. S. Sanchez, B. Wang, A. Bansil, F. Chou, P. P. Shibayev, H. Lin, S. Jia, and M. Z. Hasan, Science **349**, 613 (2015).
[55] A. Alexandradinata, Z. Wang, and B. A. Bernevig, Phys. Rev. X **6**, 021008 (2016).
[56] M. Taherinejad, K. F. Garrity, and D. Vanderbilt, Phys. Rev. B **89**, 115102 (2014).
[57] D. Gresch, G. Autès, O. V. Yazyev, M. Troyer, D. Vanderbilt, B. A. Bernevig, and A. A. Soluyanov, Phys. Rev. B **95**, 075146 (2017).
[58] L. Fu and C. L. Kane, Phys. Rev. B **74**, 195312 (2006).
[59] R. Yu, X. L. Qi, A. Bernevig, Z. Fang, and X. Dai, Phys. Rev. B **84**, 075119 (2011).
[60] A. A. Soluyanov and D. Vanderbilt, Phys. Rev. B **83**, 235401 (2011).
[61] A. Alexandradinata, X. Dai, and B. A. Bernevig, Phys. Rev. B **89**, 155114 (2014).
[62] A. Alexandradinata and B. A. Bernevig, Phys. Rev. B **93**, 205104 (2016).
[63] J. Höller and A. Alexandradinata, arXiv:1708.02943.
[64] WTe_2 is symmetric under a screw ($\tilde{\mathfrak{s}}$), which is composed of a twofold rotation ($\mathfrak{c}_{2z}$) and a half-lattice translation in $\vec{z}$. The group algebra involving $\tilde{\mathfrak{s}}$ is isomorphic to one involving $\mathfrak{c}_{2z}$, if we restrict ourselves to the $k_z = 0$ plane.
[65] J. M. Luttinger and W. Kohn, Phys. Rev. **97**, 869 (1955).
[66] J. Zak, Phys. Rev. Lett. **54**, 1075 (1985).
[67] See Supplemental Material at http://link.aps.org/supplemental/10.1103/PhysRevLett.119.256601 for the tight-binding parameters.
[68] M. V. Berry and K. E. Mount, Rep. Prog. Phys. **35**, 315 (1972).